The TaCslA12 gene expressed in the wheat grain endosperm synthesizes wheat-like mannan when expressed in yeast and Arabidopsis

Yves Verhertbruggen, Axelle Bouder, Jacqueline Vigouroux, Camille Alvarado, Audrey Geairon, Fabienne Guillon, Mark Wilkinson, Fabian Stritt, Markus Pauly, Mi Yeon Lee, et al.

Version of Record: https://www.sciencedirect.com/science/article/pii/S0168945220302995
Manuscript_03c96caf5418f0a7ed73049254b942e0

The *TaCslA12* gene expressed in the wheat grain endosperm synthesizes wheat-like mannan when expressed in yeast and Arabidopsis.

Yves Verhertbruggen[1], Axelle Bouder[1], Jacqueline Vigouroux[1], Camille Alvarado[1], Audrey Geairon[1], Fabienne Guillon[1], Mark D. Wilkinson[2], Fabian Stritt[3], Markus Pauly[3], Mi Yeon Lee[4], Jenny C. Mortimer[4], Henrik V. Scheller[4,5], Rowan A.C. Mitchell[2], Catalin Voiniciuc[3,6], Luc Saulnier[1] and Anne-Laure Chateigner-Boutin[1]

1 INRAE, UR BIA, F-44316 Nantes, France

2 Rothamsted Research, West Common, Harpenden, Hertfordshire AL5 2JK, UK

3 Institute for Plant Cell Biology and Biotechnology, Heinrich Heine University Düsseldorf, 40225 Düsseldorf, Germany

4 Joint BioEnergy Institute, Lawrence Berkeley National Laboratory, Berkeley, CA 94720, USA

5 Department of Plant and Microbial Biology, University of California, Berkeley, CA 94720, USA

6 Independent Junior Research Group–Designer Glycans, Leibniz Institute of Plant Biochemistry, 06120 Halle (Saale), Germany

Corresponding author : **Anne-Laure Chateigner-Boutin**

INRAE-BIA-PVPP Rue de la Géraudière BP71627 44316 Nantes Cedex 3 France

anne-laure.chateigner-boutin@inrae.fr

Abstract

Mannan is a class of cell wall polysaccharides widespread in the plant kingdom. Mannan structure and properties vary according to species and organ. The cell walls of cereal grains have been extensively studied due to their role in cereal processing and to their beneficial effect on human health as dietary fiber. Recently, we showed that mannan in wheat *(Triticum aestivum)* grain endosperm has a linear structure of β-1,4-linked mannose residues. The aim of this work was to study the biosynthesis and function of wheat grain mannan. We showed that mannan is deposited in the endosperm early during grain development, and we identified candidate mannan biosynthetic genes expressed in the endosperm. The functional study in wheat was unsuccessful therefore our best candidate genes were expressed in heterologous systems. The endosperm-

specific *TaCslA12* gene expressed in *Pichia pastoris* and in an *Arabidopsis thaliana* mutant depleted in glucomannan led to the production of wheat-like linear mannan lacking glucose residues and with moderate acetylation. Therefore, this gene encodes a mannan synthase and is likely responsible for the synthesis of wheat endosperm mannan.

Keywords

Wheat grain, developing endosperm, cell walls, mannan, heterologous expression

Abbreviations

AIR: alcohol insoluble residues, AKI: alkaline insoluble, AX: arabinoxylan, BIFC: bimolecular fluorescence complementation, Csl: cellulose synthase-like, °DAF: Celsius degrees per day after flowering, DP: degree of polymerization, DUF: domain of unknown function, GC: Gas chromatography, GT: glycosyltransferase, HPAEC-PAD: high-performance anion-exchange chromatography coupled with pulsed electrochemical detection, MALDI: matrix-assisted laser desorption/ionization, MLG: mixed-linkage glucan, MS: mass spectrometry, MSR: mannan synthesis related, TM: triple mutant, TMD: transmembrane domain, TOF: time-of-flight, WT: wild type.

1. Introduction

Wheat *(Triticum aestivum)* is a major crop cultivated worldwide to produce grains that feed humans and animals. The wheat grain is a dry fruit containing a single seed with an embryo and a specialized tissue, the endosperm, where storage compounds are stored to provide energy necessary for the germinating seedling. This endosperm tissue is also highly valuable for different industries including starch, bread, pasta, and brewing.

The cereal grain develops from the fertilized ovary and undergoes a precise program of development which has four stages: syncytium, cellularization, differentiation and maturation (reviewed in [1]). In the syncytium stage, the wheat endosperm consists of dividing nuclei and cytoplasm but is devoid of cell walls. The first cell walls are formed at the beginning of the cellularization stage and subsequently cells begin to undergo mitoses. Endosperm differentiation leads to the emergence of the central starchy endosperm (storage tissue), and a peripheral layer

of aleurone cells, some of which face the ventral vascular bundle forming specialized transfer cells involved in nutrient and water uptake [2].

Cell wall polysaccharides comprise a minor fraction of the cereal starchy endosperm, typically about 5% dry weight in the mature seed. Wheat endosperm cell wall polysaccharides have been studied for more than 50 years, but very recently their composition and structure have been revised. The cell wall polysaccharide composition in mature wheat endosperm is now reported as 60-65% arabinoxylan (AX), 20-22% cellulose, 15% mixed-linkage glucan (MLG), 4-7% mannan with traces of pectin and xyloglucan [3,4,5]. The structure and function of cereal AX and MLG have been well-characterized (for a review, see [6]), and more recently, we have elucidated the structure of wheat endosperm mannan [5].

Mannan-type polymers found in plant include: linear mannan, with a backbone exclusively made of β-1,4-linked mannose residues and no or little substitution, galactomannans, with the same backbone but harboring α-1,6-linked galactose substitutions, and glucomannans and galactoglucomannans with backbones made of mannose and glucose [7,8]. The structure of mannan influences its properties such as its crystallinity, solubility, viscosity, gel-forming and film-forming abilities, water absorptivity, and thickening (for a review, see [9]). Substitutions were suggested to prevent polymer aggregation [10] or control interaction with other polymer [11]. Thus, mannan structure both has an impact *in planta* and affects how extracted mannans are used in various industries. Wheat endosperm mannans are linear mannans that are weakly acetylated [5]. Linear mannans are usually insoluble as observed, for example, in ivory nuts [12,13], but backbone acetylation may confer solubility in aqueous solution [9].

Like most hemicelluloses, mannans are synthesized in the Golgi apparatus and then are secreted to the cell wall via plasma-membrane fused vesicles [14]. To date five families of proteins have been reported to be involved in mannan synthesis: carbohydrate active enzymes (CAZY; www.cazy.org) glycosyltransferase (GT) 2 cellulose synthase-like (Csl) family A [15,16,17] and D [18,19,20], the GT34 mannan galactosyltransferases [21,22], the GT106 mannan synthesis related proteins (MSR) [23,24] and the domain of unknown function (DUF) 231 / trichome birefringence like (TBL) family [25]. Several CslA proteins from different plant species have been demonstrated to synthesize mannan and glucomannan *in vitro* after heterologous expression and purification from transgenic soybean cells, insect cells, or the yeast *Pichia pastoris* (named in the rest of the text as Pichia) [15,26,27]. Recently, Voiniciuc et al. [24] engineered Pichia cells to produce and secrete β-1,4-mannan polysaccharides by expressing the *Arabidopsis thaliana* (named in the rest of the text as Arabidopsis) AtCslA2 alone, or glucomannan by co-expressing AtCslA2 and AtMSR1. Therefore, MSR proteins are cofactors modulating the structure of the mannan polymer synthesized by CslA enzymes, and different effects were observed depending on the CslA and

MSR investigated [24]. The overexpression of AtCslDs in tobacco has been shown to modulate the production of mannan [19]. However, CslD proteins have also been reported to synthesize β-1,4-glucan [28,29]. Proteins containing the DUF 231 domain were shown to be responsible for mannan *O*-acetylation [25]. Transcriptomic [30,31,32] and proteomic studies [33] conducted on developing wheat grains have led to the identification of wheat proteins potentially involved in mannan metabolism, including several CslAs and CslDs. Acetyl esterase and glycosyl hydrolases that include mannanase, mannosidase, galactosidase and glucosidase are proteins involved in the hydrolysis and modification of mannan. Several of these proteins have been identified in cereal grains during germination [12]. Although proteins might regulate the structure and the accumulation of mannan in the cereal endosperm, there is currently no evidence to support these hypotheses in wheat grain. No changes in the structure of mannan were observed in the developing endosperm of wheat [5] where no mannan-related glycosyl hydrolases have been formally identified [33,34]. Heterologous expression [15,24] and mutant analysis [17] have greatly contributed to our knowledge of mannan metabolism and function in plants.

It has been reported that the presence of mannan is ubiquitous in the cell walls of plant tissues where it has a structural function. It is widely accepted that mannans and glucomannans are highly conserved throughout plant evolution [7,12]. Moreover, several plant species develop specialized tissues where mannan is stored as reserves of energy. This is the case of the corm of *Amorphophallus konjac* (konjac) which contains 49-60% of glucomannan [35] and of the seed endosperm of several Fabaceae species such as *Cyamopsis tetragonoloba* (guar) or *Cassia grandis* that contains 50% galactomannans [36,37,38]. In Arabidopsis, mannan has been shown to have a fundamental role as certain mutant plants lacking mannan or glucomannan are either barely viable or embryo lethal [17,19]. Furthermore, it has been suggested that mannan is involved in zygotic embryogenesis, oligosaccharide signaling and cell differentiation [16].

Here, we investigated the biosynthesis and function of wheat mannan, a polysaccharide that is synthesized and deposited in the cell walls of the developing wheat grain, especially in the endosperm tissue.

2. Material and methods

2.1. Plant material

Hexaploid (AA,BB,DD) wheat (*Triticum aestivum* L.) cv Recital were grown in pots in controlled glasshouses in INRAE Le Rheu (France) under natural day light. Individual spikes were tagged at flowering. Development stages were assessed by the thermal time method, by calculating the cumulated average temperature per day elapsed since flowering (°Celsius per day after flowering, °DAF). The two basal grains of the spikelets located in the middle of the spikes were harvested at different stages of development.

Arabidopsis thaliana Columbia-0 (Col-0) and triple mutant (TM) *csla2/csla3/csla9* [17] seeds were sown on soil and grown as previously described [39]. Tobacco plants (*Nicotiana tabacum* and *Nicotiana benthamiana)* were cultivated as in [33].

2.2. Immunolabeling and histological staining

Grain samples were fixed and embedded as described in [3]. Cross-sections were made in the equatorial region of the grains using an ultramicrotome (UC7, Leica) and the sections were stained using toluidine blue-O as described in [40]. Other sections were used for immunolabeling experiments where the procedure was performed as described in [3]. The antibodies used were LM21 and LM22 (dilution 1:5; [41]), which recognize mannan polysaccharides and oligosaccharides (DP2-DP5). Whereas LM21 displays a wide recognition of mannans, gluco- and galactomannans, LM22 does not detect galactomannans.

2.3. Sequence-based identification of the wheat candidate genes

The tentative full-length sequences of *TaCslD2*, *TaCslA7* and *TaCslA12* were originally obtained by assembling wheat EST contigs, wheat Chinese Spring genomic contigs, and RNAseq sequences [30]. The sequence assemblies were compared to nucleotide sequences contained in the NCBI database using the BlastN sequence alignment program (restricted to Poaceae), and aligned to the best hits from *Hordeum vulgare* and *Brachypodium distachyon.*

The cDNA sequences were then isolated from the developing endosperm of wheat grain (cv Recital). RNA isolation, cDNA synthesis and PCR were performed as described in [33]. Total RNA was isolated from manually dissected endosperm of wheat grains at 250°DAF using the phenol-chloroform method [33]. RNA was treated twice with DNase (Qiagen) and then purified through the RNeasy MinElute Cleanup kit (Qiagen), following the manufacturer's recommendations. Reverse

transcription was carried out with 2 µg of total RNA primed with random hexamers using the Transcriptor First Strand cDNA synthesis kit (Roche).

cDNA was amplified by PCR using a high fidelity Q5 DNA polymerase (New England Biolabs) with the primers listed in **Table S1**. PCR products were cloned into pCR-BluntII-Topo vector (Thermofisher) and sequenced.

2.4. In silico analysis of the wheat sequences

Sequences were translated in silico using the ExPASy Translate tool (https://web.expasy.org/translate/). Nucleotide and protein sequences were aligned using Clustal Omega (1.2.4) and Multalin (http://multalin.toulouse.inra.fr/multalin/). Transmembrane domains were predicted using TMHMM 2.0 (http://www.cbs.dtu.dk/services/TMHMM/). Signal peptide and cleavage site prediction was obtained with TargetP 1.1 (http://www.cbs.dtu.dk/services/TargetP/) for Plant. The expression profiles of the targeted genes were obtained from microarray experiments [31,32], RNAseq experiments [30] and from data available at the PlaNet expression database (http://aranet.mpimp-golm.mpg.de/index.html) [42] and at www.wheat-expression.com [43,44]. The cDNA sequences were also aligned against the recently released gene models for wheat Chinese Spring (IWGSC 2018) (Ensembl Wheat release 47 - April 2020) available at https://plants.ensembl.org/Triticum_aestivum/Info/Index.

2.5. Expression of wheat genes in tobacco plants

Wheat cDNAs were amplified using primers containing attB sequences for gateway recombination **(Table S1).** For subcellular localization studies, the binary pK7FWG2 and pK7RWG2 vectors containing the 35S promoter of cauliflower mosaic virus (CaMV) and the eGFP (enhanced green fluorescent protein) or mRFP (monomeric red fluorescent protein) respectively were used to generate C-terminal fusions. The inserted genes were *TaCslD2, TaCslA7* and *TaCslA12* and the Golgi marker, sialyltransferase (ST; [45]), and the endoplasmic reticulum (ER) marker, dihydrosphingosine phosphate lyase 1 (DPL1; [46]). Co-transformation experiments were conducted to observe co-localization. For bimolecular fluorescence complementation (BIFC) experiments, the vectors pBIFP-1 and pBIFP-4 containing the N-terminal part and C-terminal parts of the fluorescent eYFP (enhanced yellow fluorescent protein) respectively were used to generate C-terminal fusions [47]. Interacting MADS-box transcription factors DEFICIENS and GLOBOSA [48] were used as positive controls. Agroinfiltration of tobacco leaves and observations using a

confocal microscope were carried out as described in [33]. *N. tabacum* was used for subcellular localization studies and *N. benthamiana* transformed with the silencing inhibitor P19 was used for BIFC experiments as in [47].

2.6. Expression of wheat genes in Pichia pastoris

The expression of *CslA* genes in Pichia was performed essentially as described in [24]. Plant cDNAs were cloned using the EasySelect Pichia Expression Kit (Invitrogen), according to the manufacturer's manual. The cDNA sequences, including stop codons, were inserted using restriction enzymes in the multiple cloning site of the pPICZ B vector (Invitrogen) and transformed in *Escherichia coli* TOP10F' cells for propagation. The primers used to amplify the genes of interest are listed in **Table S1.** The resulting pPICZ B + *CslA* plasmids were verified by colony PCR and sequencing using the vector- and gene-specific primers listed in **Table S1.** Linearized plasmid DNA (150 ng) was used to transform Pichia X-33 cells by electroporation [49]. Transgenes were integrated into the *pAOX1* region of the Pichia genome via homologous recombination, and verified by yeast colony PCR.

Multiple independent Pichia transformed colonies were cultured in 24-well plates for around 60 h and the *pAOX1* promoter was then induced by the addition of methanol as described in [24]. After 24 h of methanol induction, Pichia cells were transferred to 2 mL tubes and collected by centrifugation. Alcohol Insoluble residue (AIR) containing yeast wall material was obtained and mannosylated proteins were removed with 1 M NaOH for 60 min at 75°C and 1,400 rpm in a thermomixer (Eppendorf) as described in [24]. Alkaline-insoluble (AKI) polysaccharides were pelleted at 20,000 g for 2 min and washed with water. The resulting AKI material was resuspended in 600 µL of water by mixing at 30 Hz for 2 min 30 s using a ball mill, and used immediately for enzymatic digestion or stored at 4°C.

The monosaccharide composition of the AKI polymers was determined via high-performance anion-exchange chromatography coupled with pulsed electrochemical detection (HPAEC-PAD), as previously described [22,50], on a 940 Professional IC Vario ONE/ChS/PP/LPG instrument (Metrohm) equipped with a CarboPac PA20 guard and analytical column.

For enzymatic characterization, AKI polymers were incubated with 1 U of *endo*-1,4-β-mannanase (Megazyme, E-BMABC) for 30 min at 40°C and 1,000 rpm in a thermomixer (Eppendorf). Afterwards, the samples were centrifuged for 2 min at 20,000 g, and 100 µL of the

supernatant was used to quantify the amount of sugar released. Total hexose sugars were quantified using the anthrone assay [51].

Glycosidic linkages in Pichia material were analyzed by gas chromatography–mass spectrometry (GC-MS) following derivatization of partially methylated alditol acetates as described in [52], with modifications as described in [53]. Carbohydrates were separated using a 5977A Series GC-MS system (Agilent) equipped with a SP-2380 capillary column (Supelco). Carbohydrate peaks were annotated based on their retention time and ion spectra relative to standards.

2.7. Expression of wheat genes in Arabidopsis thaliana

The vector used for Arabidopsis transformation derived from the pIpKB1 vector [54]. The nucleotide sequence of the IRX5 promoter (*AtCesA4*) was amplified from the pTKan-pIRX5-GW [55] using the primers SpeI_AtCesa4For and AtCesa4_AscIRev (**Table S1**) and introduced by ligation after restriction using SpeI and AscI into the promoter cloning site of the pIpKB1 vector.

The Arabidopsis triple mutant (TM) *csla2/csla3/csla9* [17] was grown as described above, and transformed using the floral dip method [56]. The resulting seeds were surface sterilized and selected in Murashige and Skoog (MS) medium containing 25 µg/mL hygromycin. Seedlings from six transformed lines were then transferred to soil.

Seeds from Col-0 (WT) and TM were sown on MS medium without hygromycin and grown in the same conditions as the transformed lines. The genotype of the background line and the presence of the wheat gene was verified by extracting DNA from the lines using the fast dipstick protocol [57] and PCR performed using the primers listed in **Table S1**.

Inflorescence stems of mature plants (basal 15 cm) were harvested and stored at - 80°C. The stems were weighed, cut and incubated in 96% ethanol at 65°C for 30 min. The ethanol was removed and the stems were washed several times with 96% ethanol until the liquid stayed transparent. The samples were oven-dried at 40°C and then ground with liquid nitrogen in a freezer miller to obtain AIR.

AIR samples were hydrolyzed in 26N H_2SO_4 for 30 min at 25°C and then with 2N H_2SO_4 at 100°C for 2 h. Individual monosaccharides were then converted into alditol acetates [58] and analyzed by gas liquid chromatography as previously described [59]. The values were obtained from technical duplicate.

The mannan structure of Arabidopsis stems was studied using enzymatic fingerprinting with a recombinant *endo*-1,4-β-mannanase from *Cellvibrio japonicus* (Megazyme, E-BMACJ) as described in [5]. Briefly, 15 mg of AIR were suspended in 1 mL of distilled water and incubated at 40°C overnight with 40 U. mL^{-1} mannanase. After centrifugation, the supernatant was collected and heated for 10 min at 95°C. 200 µL was mixed with 400 µL 96% ethanol and incubated at 4°C for 4 h. After centrifugation at 13,000 g, the supernatant was collected and 200 µL of supernatant was mixed with 1.8 mL of water and filtered through a 0.45 µm filter. The oligosaccharides were analyzed by HPAEC-PAD with a Dionex Carbo-Pac PA1 column (4×250mm, Thermo Fisher Scientific) at 30°C eluted at 1 mL. min^{-1} using a linear gradient of sodium acetate from 0 to 0.1 M in 0.1 M NaOH for 30 min. They were also analyzed by matrix-assisted laser desorption/ionization (MALDI)-time-of-flight (TOF) mass spectrometry (MS) as described in [5]. The samples (1 µL) were deposited and covered by the matrix (2,5-dihydroxybenzoic acid and *N*,*N*-dimethylaniline; 1 µL) on a polished steel MALDI target plate. MALDI measurements were then performed on a rapifleX MALDI-TOF spectrometer (Bruker) operated with positive polarity in a reflectron mode, and spectra were acquired in the range of 500–2500 m/z.

3. Results

3.1. Mannan is deposited in the cell walls of the developing endosperm from the cellularization stage

The study of cell wall polymers of wheat grain revealed the presence of mannose-containing polysaccharides in the dry mature grain and in the developing grain [5,60,61,62].

Immunolabeling experiments demonstrated that mannan epitopes are predominantly detected in the walls of the wheat grain endosperm and less in the maternal outer tissues of the grain [30,62]. This heterogeneity was not as apparent in the grain tissues of rice [62] and *Brachypodium distachyon* [63]. To improve our knowledge of the physiological functions of mannan in cereal grains, we conducted immunolabeling experiments with antibodies targeting mannan epitopes on sections of wheat grains harvested at different stages of development. The aim was to refine the kinetics of mannan deposition in wheat grain and particularly to monitor its first appearance in the walls of the developing endosperm.

Two antibodies, LM21 and LM22, are commercially available to detect mannan (www.plantprobes.net). The LM21 antibody has been shown to bind to a wider range of mannan polysaccharides than the LM22 antibody [41]. In the Arabidopsis stem, mannan was barely detected when using LM22 and strongly detected with the LM21 antibody [64]. We have observed a similar result when using both antibodies on sections of developing wheat grains. Only a weak signal of fluorescence was observed in the endosperm cell walls with the LM22 antibody (**Fig. S1A**). By contrast, mannan was abundantly detected when using LM21 **(Fig. S1B).** Therefore, in all of the following experiments, we used the LM21 antibody. No mannan was detected in transverse sections of the ovary at anthesis or of grains harvested at 75°DAF, a very early stage of development that occurs within the first four days after flowering. As shown in our bright-field micrographs, it is worth to note that at 75°DAF cell walls are already present in the developing endosperm (**Fig. 1**). The LM21 mannan epitope was detected in the endosperm and in some cells of the maternal tissues from wheat grain harvested at 90°DAF (**Fig. 1**). The maternal cells labeled with LM21 are located in the nucellar projection in the crease region (**Fig. 1**). In the developing endosperm cells at 90°DAF, the LM21 epitope was strongly detected in the walls of the first cell layers bordering the endosperm cavity, and a gradient of signal intensity was observed from the ventral region of the endosperm (crease region) to the dorsal region of the endosperm (**Fig. 1**). At this developmental stage, signs of endosperm cell division are visible (see the bright-field micrographs). At subsequent stages, the LM21 antibody labels the walls of the endosperm until maturity (**Fig. S1B**).

3.2. Identification of mannan-related genes expressed in wheat grain endosperm

Since mannan is deposited during development in the nucellar projection and endosperm (**Fig.1**), tissues that are important for seed filling, it could impact grain quality. We therefore decided to isolate and study mannan-related genes expressed in wheat grain. Transcriptomic [30,31,32] and proteomic studies [33] conducted on developing wheat grain and isolated endosperms have led to the identification of wheat genes potentially involved in mannan metabolism. Our initial bioinformatics analysis of the expression profile of these genes in different organs was performed in 2013 using data from [30,31,32] and from the expression platform PlaNet (http://aranet.mpimp-golm.mpg.de/index.html) (**Table 1** and **Fig. S2**). These studies suggested that *TaCslD2, TaCslA7,* and *TaCslA12* were predominantly expressed in the developing endosperm of wheat and were therefore further characterized. More recent expression data

(www.wheat-expression.com) revealed that while *TaCslA12* really appears to be specifically and highly expressed in the wheat developing grain, both *TaCslA7* and *TaCslD2* have significant expression in other tissues in addition to endosperm **(Fig. S2).**

The cDNA sequence of wheat *TaCslD2*, *TaCslA7* and *TaCslA12* was obtained from RNA isolated from wheat developing endosperm (cv Recital). The sequences were first aligned with the available sequences of related species to verify their coverage. Notably *TaCslA7*, *TaCslA12* and *TaCslD2* sequences were aligned to barley (*Hordeum vulgare)* AK359952.1, AK376872.1 *and* BAJ93918.1, respectively. An open reading frame was identified for each sequence and was amplified for subsequent cloning.

We analyzed the sequences of the *TaCslD2*, *TaCslA7* and *TaCslA12* cDNA we originally obtained and we compared them to the coding sequences of the wheat gene models that were recently released (IWGSC 2018, release 47, April 2020).

The protein sequences derived from *TaCslA12* and *TaCslA7* cDNAs in our study and those predicted for the Chinese Spring wheat cultivar TraesCS2B02G560100.1 and TraesCS2D02G163000.2, respectively, are almost identical. The cloned cDNAs are encoded by the B genome for TaCslA12 and the D genome for TaCslA7. TaCslA12_B and TaCslA7_D proteins contain the conserved sequences among polymerizing beta-glycosyltransferases (aspartyl residues as well as the motif QXXRW (Gln-X-X-Arg-Trp) (**Fig. S3A**) and the DxD motif of GT (the DXD motif in the catalytic site interacts with the phosphates of the NDP-sugar via a metal ion [65]). However, when compared to other CslA proteins and in particular to the mannan synthase (ManS) CslA of guar, konjac and Arabidopsis (**Fig. S3A**), we realized that the TaCslA7 sequence was longer in the N-terminal region. That region is not conserved among CslAs. Prediction tools for subcellular location and signal peptide prediction were applied. Putative cleavage sites were found using TargetP for TaCslA7, TaCsl12 and AkCslA3 (**Fig. S3A**). Thus, CslA polypeptides might contain N-terminal peptides cleaved in the mature proteins. This would explain why Dhugga et al. [15] and Liepman et al. [26] observed that CslA proteins displayed an apparent lower molecular weight than predicted from the corresponding peptide sequence upon migration in gels. N-terminal cleavage of TaCslA12 and TaCslA7 would remove one transmembrane domain (TMD). The TMD prediction program TMHMM predicted that the long sequence between the N-terminal TMD and the four C-terminal TMDs, which contains the active site would be located in the Golgi lumen (inside) with or without cleavage (**Fig. S3B)**. According to the gene model in Ensembl wheat (release 47 April 2020), there are 2 splicing variants for *TaCslA7_D*. TraesCS2D02G163000.2 encodes a protein of 581 amino acids and TraesCS2D02G163000.1 encodes a protein of 353 amino acids, lacks an exon in N-terminus and

therefore contains only the four C-terminal TMDs. Homoeologous sequences were identified in the Chinese Spring genome for TaCslA12 (TaCslA12_A: TraesCS2A02G530900 and D: TraesCS2D02G532800) and TaCslA7 (TaCslA7_A: TraesCS2A02G157100 and B: TraesCS2B02G182700).

The cloned TaCslD2 cDNA sequence was used to identify the best Blast hits in Chinese Spring wheat. Two very close sequences were identified in chromosome 7 and 4, each in only one genome. Best hits were TraesCS7D02G029700.1 (genome D) and TraesCS4A02G456300.1 (genome A) (**Table 1**). The protein sequence (**Fig. S3C**) contained the conserved sequence for polymerizing beta-glycosyltransferases QXXRW (Gln-X-X-Arg-Trp) and the DxD motif, TMDs, and it bears a Zinc finger domain (IPR013083) which could be involved in protein-protein interaction.

3.3. The heterologous expression of wheat TaCslA12-B leads to the production of wheat-like mannan

We attempted to produce knocked-out or down-regulated wheat lines for the *TaCslA7*, *TaCslA12* and *TaCslD2* genes. Regardless of the strategy trialled, these attempts were unsuccessful ([31] and data not shown). Therefore, as an alternative approach to study these genes, we expressed the wheat mannan-related genes in heterologous systems.

3.3.1. Heterologous expression in tobacco leaf

To verify the subcellular localization of the proteins, the coding sequence was cloned in fusion with a fluorescent reporter gene and introduced into tobacco by leaf agroinfiltration. Fusion proteins were detected for the three constructs by confocal microscopy. TaCslA7 and TaCslA12 fusion proteins were observed as small fluorescent dots which co-localized with the Golgi marker sialyltransferase (**Fig. 2**). These results indicate that TaCslA7 and TaCslA12 are localized in the Golgi apparatus. This is in accordance with previous results for CslA proteins from other species and with the fact that mannan biosynthesis occurs in the Golgi apparatus [15]. However, the TaCslD2 fusion protein was observed as a network and co-localized with the ER marker. No Golgi signal was detected for TaCslD2 alone when fused to either GFP or RFP as C-terminal or N-terminal fusion. A co-transformation experiment was conducted with TaCslD2 and TaCslA12. We observed that the subcellular localization differs when the fusion proteins were expressed alone or together in tobacco leaf. Fluorescent signals for both TaCslD2 and TaCslA12 were seen as both dots and networks, with partial overlays of the signals (**Fig. 2**). One potential explanation for the

changed localization is that the proteins interact. To test this, BIFC experiments were carried out. TaCslD2 and TaCslA12 and positive controls were fused in their C-terminal region to both N- and C-terminal regions of the split fluorescent YFP and introduced into tobacco leaves. Fluorescence signals marking the formation of a full functional YFP by close co-localization of the tested partners were only obtained for the positive controls **(Fig. S4)**. No significant signal was observed when TaCslD2 and TaCslA12 were co-infiltrated. Moreover, BIFC experiments were also conducted with either TaCslD2 or TaCslA12 infiltrated as two fusion proteins with N- and C-terminal regions of the YFP. No significant signal indicative of homomultimeric interactions was observed **(Fig. S4)**.

3.3.2. Heterologous expression in the yeast Pichia pastoris

Recently the yeast Pichia showed its great utility as a system for testing the heterologous activity of plant mannan synthesis genes [24]. We took advantage of this system and transformed Pichia with the *TaCslA7* and *TaCslA12* coding sequences. Pichia expressing the AkCslA3 glucomannan synthase from konjac [24,27] was used as positive control and yeast containing no heterologous enzyme (empty vector) served as negative control. After culture and methanol induction, alkaline-insoluble polysaccharides were isolated and screened for the presence of mannan using an endo-β-1,4-mannanase. The colorimetric anthrone assay showed that the content of hexose sugars released by mannanase digestion significantly increased in Pichia expressing *AkCslA3* or *TaCslA12* (**Fig. 3**). Unlike *TaCslA12* and *AkCslA3*, the *TaCslA7* construct was not sufficient for mannan production in Pichia. Permethylation experiments identified an enrichment in 1,4-mannosyl linkages in the cell wall polymers of both the AkCslA3 and the TaCslA12 yeast strains. However, the 1,4-glucosyl linkage content was only significantly increased by the expression of *AkCslA3* (**Fig. 3**). These assays suggest that, when expressed alone in *P. pastoris*, the wheat *CslA12* gene produced β-1,4-mannan chains that do not contain glucose moieties. This is consistent with the mannan structure found in the cell walls of the mature and developing wheat endosperm [5].

3.3.3. Heterologous expression in a triple mutant of Arabidopsis *devoid of mannan in its stem*

The wheat *TaCslA7_D* and *A12_B* cDNAs were also expressed in Arabidopsis. The coding sequences were introduced in a triple mutant (TM) *csla2/csla3/csla9* which lacks mannan in the cell wall of its stem [17] but grows phenotypically normally unlike the embryo-lethal *csla7* mutants

[66]. The wheat gene was introduced under the control of the promoter of *AtCesA4/irx5,* which targets the expression in the secondary cell walls of the stem [55]. The strong 35S promoter was avoided so as to not disturb embryogenesis and seedling development. Selection of transformed lines by growth on hygromycin and PCR targeting the wheat insert led to the identification of several independent transformed lines for TaCslA12 but none were recovered for TaCslA7. No phenotypic differences were noticed between Col-0 (WT), TM and the transformed TM lines. Alcohol insoluble polysaccharides were isolated and analyzed by chemical hydrolysis, alditol acetate derivatization and GC analysis to study the cell wall composition of the mature stems. The mannose content of WT stems reached about 3.7% of total neutral sugars and no mannose was detected in the TM line. In two independent TM lines transformed with the *irx5::TaCslA12* construct (71.1 and 72.1), mannose was detected and reached a percentage of total neutral sugars similar to that of the WT (**Table 2**). Thus, the *TaCslA12_B* gene is functional in Arabidopsis stem and leads to the production of mannan.

Alcohol insoluble polysaccharides of WT, TM and TM transformed with the pro*irx5::TaCslA12* (71.1 and 72.1) were incubated with a recombinant *endo*-1,4-β-mannanase and the released oligosaccharides were compared by HPAEC profiling. Several peaks were obtained in the WT sample not treated with endo-mannanase, and hence those peaks were considered non-specific to the mannanase hydrolysis (**Fig. 4**). Commercial mannose, manno-oligosaccharides (DP2 to DP6) and endo-mannanase-treated glucomannan from konjac were used as standards to identify the peaks resulting from the action of the endo-mannanase. The profile of the mannanase-treated TM contained only small peaks, among which two had similar retention time to mannose and mannobiose. This was also observed in the chromatogram of the untreated WT (**Fig. 4**). The profile of the mannanase-treated WT samples and that of the lines 71.1 and 72.1 contain peaks that can be attributed to mannose and manno-oligosaccharides (DP2 to at least DP4). The profile of konjac and WT Arabidopsis samples contains additional glucomannan-specific peaks, that are not present in the profile of the complemented lines 71.1 and 72.1 (**Fig. 4**). Arabidopsis stems contain glucomannan in their secondary walls [67]. These results suggest that the TaCslA12 protein introduced into Arabidopsis produced mannan but not glucomannan, and this is in agreement with the result obtained in *Pichia*. Differences in peak area were observed. For example, most manno-oligosaccharides of small DP showed proportionally larger peaks in the 71.1 and 72.1 samples as compared to the WT. Mass spectrometry experiments were conducted to monitor mannan acetylation in WT and in complemented lines. Indeed, one possible explanation for the lower signal for manno-oligosaccharides of small DP could be that mannans in WT Arabidopsis are less easily hydrolyzed by the mannanase due to a higher level of acetylation. **Fig. 5** shows the mass profile of the oligosaccharides generated by the endo-mannanase from

stems of a WT and a complemented line (72.1). In the m/z range investigated, the detected oligosaccharides were oligo-hexose of DP3 (Hex-DP3+K^+ m/z 543.14) to DP15 (Hex-DP15+K^+ m/z 2487.77). The mass profiles identified more oligo-hexose of higher DP in WT when compared to the complemented line. Typical mass spectrometric signatures of acetylation (addition of m/z 42.01 and its multiple) were present. While *O*-acetylation was found in line 72.1, extensive acetylation was revealed in the WT sample. Interestingly very high signals were found in WT for Hex-DP5+K^+ + 2 acetyl-substituents (m/z 951.25) and Hex-DP6+K^+ + 2 acetyl-substituents (m/z 1113.28).

4. Discussion

Recently, we have shown that mannan in wheat grain endosperm are relatively short chains of β-1,4-linked mannose residues that are weakly acetylated. We have also observed that the structure of mannan does not vary during grain development [5]. To improve our knowledge of this polysaccharide in wheat, the deposition pattern of mannan, the cell machinery involved, and the physiological function and importance of wheat endosperm mannan were investigated.

The work described here has revealed new information about cell wall formation during cereal grain development. Our immunolabeling assays suggest that mannan is involved in the early development of endosperm cells as it is first detected in their walls during the cellularization stage. However, mannan was absent in the first cell walls formed in the endosperm. At 75°DAF, prior to the occurrence of mannan, immunolabeling experiments have shown that the endosperm cell walls contain callose and mixed-linkage glucans [68]. Arabinoxylan, the main polysaccharide of mature endosperm cell walls, is detected from 90°DAF in the grain cell walls, and appears visible from 150°DAF in the endosperm cell walls [69]. The precise order of deposition of the different cell wall polymers is likely important for the correct establishment of the endosperm cell walls and possibly for the functional differentiation of the endosperm cell types (aleurone cells, transfer cells, starchy endosperm).

To study the impact of mannan in wheat endosperm, we targeted members of the GT2 CslD and CslA families that were demonstrated to be related to mannan synthesis in other species [15,18]. While the activity of CslDs is still under debate, it has been firmly demonstrated that CslA proteins synthesize linear mannan and glucomannan. The targeted genes were well expressed in the developing wheat endosperm as revealed by previous transcriptomic and proteomic studies [33,30]. We attempted to obtain wheat mutants and transformants with altered mannan content in their endosperm, but our efforts have been unsuccessful.

We therefore studied the selected wheat *Csl* genes heterologously in several systems. In tobacco leaves as C-terminal GFP fusion protein, we found that TaCslD2 was localized in the ER when expressed alone. This does not support a direct role in mannan synthesis. However, different subcellular localizations have been observed for other CslD proteins: ER, Golgi and plasma membrane [28,70,71]. These studies showed that the observed localization varied for the same CslD protein depending on the cell type or fusion type (C-terminal or N-terminal fusion). Moreover, while several studies have demonstrated that CslD proteins have an impact on mannan content [19,73], there is an accumulation of evidence that suggests that this may be indirect. Meanwhile, many studies suggest a role for CslD proteins in the synthesis of cellulose [28,29,71,72,73].

TaCslA7 and TaCslA12 were located in the Golgi as expected for mannan synthases. The TaCslA7 protein fused with the GFP was expressed and targeted to the expected subcellular location. However, the same coding sequence transformed into *Pichia pastoris* was not able to produce mannan polymers in the yeast wall. Numerous reasons could explain this discrepancy. The long, uncleaved TaCslA7 might not fold correctly hindering its activity. Alternatively, Voiniciuc et al. [24] showed that some CslA proteins such as the *Coffea canephora* (Cc) MANS1 required a CcMSR1 cofactor to synthesize mannan in Pichia. It is thus possible that TaCslA7 requires a wheat cofactor in Pichia. It is interesting to note that the ortholog of *AtMSR1* in Chinese Spring wheat is expressed in the same tissues as *TaCslA7* (**Fig. S2**).

In Pichia, TaCslA12_B expressed alone produced a wheat-like linear β-1,4-mannan. In Arabidopsis TM depleted in glucomannan, the introduction of TaCslA12_B under the control of a promoter targeting stem tissues restored the WT mannose level. The structure of the mannan polysaccharides incorporated in cell walls is apparently different from that of the WT Arabidopsis glucomannan as revealed by enzymatic fingerprinting. The structure is also slightly different from that obtained from mature wheat endosperm since endo-mannanase fingerprinting produced profiles with only mannose, mannobiose and traces of mannotriose [5]. Mass spectrometry profiling showed that the mannan produced by TaCslA12_B in Arabidopsis stems are significantly acetylated but to a lower extent than the WT Arabidopsis glucomannan. Therefore, it seems that the Arabidopsis glucomannan acetyltransferase is versatile enough to acetylate linear mannan. In wheat endosperm, traces of acetylation were detected in mannan and associated with hexotriose [5]. The TaCslA12_B mannan in Arabidopsis therefore appears to be more acetylated than the wheat endosperm mannan. The remaining mannotriose and larger DP oligosaccharides likely reflect the recalcitrance to hydrolysis of acetylated mannooligosaccharides.

Many questions remain unanswered. First concerning the GT2-Csl superfamily and the mannan biosynthesis machinery. Several genome-wide studies of GT2 families have been conducted over the last decades in Arabidopsis [74], rice [75], wheat [76] and recently in 46 species [77]. Functions have been assigned to many Csl families in hemicellulose backbone synthesis. However, a recent publication revealed that not all Csl proteins are involved in cell wall synthesis. An ER localized Csl protein was shown to glucuronidate specialized metabolites (triterpenoid saponins) [78]. This example shows that caution should be exercised before predicting the function of a protein on the basis of its sequence homology and that experimental evidence is needed.

Csl families are multigene families. In addition, many genes exist as variants. This is particularly true for polyploid species such as bread wheat. Kaur et al. [76] identified 108 genes in the wheat Csl families, each with two to three homeoalleles (subgenomes A, B, D) and for many of them 2 to 3 splice variants. Some of the genes we studied here were not annotated in Kaur et al. [76], and therefore the total number of *Csl* genes will increase as improved wheat genomes and transcriptomes become available. It is not clear why plant genomes contain so many *Csl* genes even within the same Csl family since to date the characterized members of the same Csl family have shown similar enzymatic activities. For the CslA family: 9 genes are present in the genome of Arabidopsis and 9 in rice [75]. According to the Ensembl wheat (Chinese Spring wheat genome release 47 April 2020), *CslA* genes have 52 paralogue sequences (16 paralogues for A genome, 18 paralogues for B genome, 18 paralogues for D genome). After elimination of closely related *CslC* family members, the number is reduced to 35 (12 genes, **Table 1**). Kaur et al. [76] explored publicly available expression data for wheat *Csl* genes in which only some of these genes would show tissue specific expression in wheat. One would expect some organ and/or tissue even cell type specificity and also developmental regulations. Transcriptomic and proteomic experiments with better spatial and temporal resolution are required for wheat to elucidate this question.

In the developing wheat endosperm, previous experiments showed that five *CslA* genes are expressed and that *TaCslA12* and *A7* are the most highly expressed [30]. Mining transcriptome databases, *TaCslA12* was found to be the only wheat *CslA* gene specifically expressed in the wheat grain (**Fig. S2**). One explanation for producing 5 CslA proteins in the same tissue is that several CslA proteins might form homo/heteromultimeric complexes as this has been observed for example for the biosynthesis complex involved in cellulose, xylan, xyloglucan, homogalacturonan and arabinan synthesis [79,80,81,82,83]. This is a point to further investigate for CslAs. Our data show that at least TaCslA12 can function on its own in Pichia. Our BIFC experiments failed to reveal homodimeric complex. One can envision that even if TaCslA12 has the ability of acting alone (as a monomer or an homomultimeric complex) in mannan synthesis, it might act more

efficiently in heteromeric complexes to increase production rate or chain length as described for other GTs in Amos and Mohnen [84].

Another explanation for producing several CslA proteins in a same tissue would be that these CslAs might synthesize different types of mannan. That would be in accordance with the expression in the wheat grain of an orthologue of AtMSR1, which is involved in the synthesis of glucomannan [24]. However, only linear mannan with no glucose and no substitution (other than acetylation) were detected in wheat endosperm [5]. Therefore, our data suggest that all wheat endosperm CslAs synthesize linear mannan.

Meanwhile the enzymatic role of CslD proteins is still under debate. In several species (Arabidopsis, rice and maize for instance), characterized mutants or overexpression lines altered in *CslD* genes exhibit strong phenotypes: root hair defects [85], defect in pollen tube growth [70], dwarfism, reduced organ size [87], and lethality [19]. According to Gu et al. [87] and Li et al. [86], CslDs would participate in the biosynthesis of the cell plate during cell division thus having a role in controlling organ size. Possible implication of CslDs in mannan and in cellulose synthesis were reported [18,28,29]. The CslD family is the Csl family phylogenetically closest to the CESA family, which are the catalytic proteins producing cellulose in cellulose synthase complexes [74]. Several *csld* mutants exhibit decrease in cellulose content [88,89], chimeric AtCslD3 protein containing AtCESA6 catalytic domain complemented the root hair defect of the *csld3* mutant [28]. The Arabidopsis *csld2/csld3/csld5* mutants lacked the immunolabeling of mannan epitopes found in WT interfascicular fibers [18]. In addition, tobacco microsomes isolated from plants expressing Arabidopsis CslDs incorporate more GDP-^{14}C-mannose into alcohol-insoluble polymers than the control untransformed plants [18,19].

Several studies have revealed concomitant expression of CslD and CslA proteins in tissues producing mannans. This is the case for the wheat endosperm here, for the early developing cotton fiber before accumulation of cellulose [90] and for the developing seed endosperm of guar conducted during the massive accumulation of galactomannan [73,91]. Here we showed that heterologous co-expression of TaCslD2 and TaCslA12 in tobacco leaves resulted in the co-localization of both proteins. This raises the possibility that these CslDs might act in close cooperation with CslAs.

Mannans are widespread in plant cell walls. In some species, mannan is the main hemicellulose component of cell walls. This is the case for ferns such as *Adiantum raddianum* [92] and the wood of gymnosperms [93]. Several physiological functions were attributed to mannans (reviewed in [16]). In some species, mannan is stored as reserves of energy and water [37]. In fern

roots, mannans are deposited to limit pathogen attacks [94]. Other functions were reported such as to increase tissue rigidity of seeds in tomato [37], a function in signaling (galactoglucomannan oligosaccharides) [95] and, in Arabidopsis, mannan has been suggested to function in trichome adhesion [96], pollen tube growth [66], and embryogenesis [17]. These functions depend on the fine structure of mannan and likely on its abundance. It is unclear what the physiological advantage is for wheat to produce a few percent of mannan molecules in the cell walls of its endosperm. What is the relevance of the programmed deposition order of polysaccharides in the first cell walls of the developing endosperm? And what about the relevance of the observed polarity between the ventral and the dorsal region of the endosperm? Could mannan be involved in cell differentiation? In Arabidopsis, mannan has been shown to have a fundamental role in seed development since the Arabidopsis *csla7* mutant is embryo-lethal [66]. Further studies will be required to address these questions.

Wheat mutants or variants may produce useful additional information. So far, we failed to obtain such mutants but there is no doubt that, in the future, mutagenesis and CRISPR technologies or overexpression will help to better understand the functions of mannan in wheat grain and other economically important seeds.

5. Conclusion

Mannans were detected in cell walls of the developing grain endosperm from early stages of development but not since the first appearance of endosperm cell walls. *TaCslA12* a gene preferentially expressed in the developing wheat endosperm encodes a protein located in the Golgi in plant cells where mannan synthesis occurs and, when expressed heterologously leads to the production of β-1,4-mannan in yeast and in the stem of an Arabidopsis mutant lacking glucomannan. Further studies will be needed in order to demonstrate if mannan is also essential for early cell development and grain development in wheat.

Tables:

Table 1 : Wheat *CslA* and *CslD* genes.

In red genes studied here.

Name	prot size AA	Ensembl 47 April 2020 best blast hit	Ortholog Ensembl rice	Nemeth 2010	rice ortholog	LOC_ rice	EST grain wheat	Affymetrix probe set	Expression wheat endosperm RNAseq (days post flowering) Pellny 2012						
									10	14	17	21	28	sum	rank
TaCslA12	528	**TraesCS2B02G560100.1**	Os09g0572500	A12	OsCslA12	Os09g39920	10	Ta.28315.1.S1_at TaAffx.78802.1.S1_at	639	88	31	19	33	811	14
TaCslA7	581	**TraesCS2D02G163000.2 (2)** TraesCS2B02G182700	Os07g0630900	A7	OsCslA7	Os07g43710	6	TaAffx.30043.1.S1_at TaAffx.95239.1.A1_at	198	135	191	119	125	768	15
TaCslA1	518	TraesCS6B02G197200.1	Os02g0192500	A1	OsCslA1	Os02g09930	4	TaAffx.42425.1.S1_at Ta.10065.1.S1_at	7	1	8	2	14	32	120
TaCslA3	547	TraesCS7B02G093900	Os06g0230100	A3	OsCslA3	Os06g12460	3	TaAffx.9510.1.S1_at Ta.15893.1.S1_at	20	22	27	11	11	91	87
TaCslA2	528	TraesCS6B02G135100	Os10g0406400	A2	OsCslA2	Os10g26630			21	21	20	19	16	98	83
TaCslA9	515	TraesCS7B02G295800	Os06g0625700	A9	OsCslA9	Os06g42020	1								
TaCslA11	408	TraesCS3B02G054500	Os08g0434632	A11	OsCslA11	Os08g33740									
	571	TraesCS3B02G558400 (2)	Os08g0434632												
	524	TraesCS7B02G494000	Os09g0572500												
	522	TraesCS7B02G296000	x												
	534	TraesCS3B02G540800	Os02g0744650												
	519	TraesCS7B02G296100	x												
TaCslD1	993	TraesCS7A02G331500		cslD1	OsCslD1	Os10g42750	8	Ta.9118.1.S1_at	15	6	5	2	4	32	121
TaCslD2	1188	TraesCS**7**D02G029700.1 (very close paralog TraesCS4A02g456300.1)		cslD2	OsCslD2	Os06g02180	5	Ta.9118.1.S1 TaAffx.105670.1.S1	176	78	39	42	52	386	24
				cslD4	OsCslD4	Os12g36890	5	TaAffx.118567.1.A1							

Table 2. Individual neutral sugars composition of cell walls for the mature stems of Arabidopsis lines (% individual neutral sugar in Alcohol Insoluble Residue)

Sugar/sample	WT1	WT2	TM1	TM2	71.1	72.1
Rhamnose	1.25 +/- 0.15	1.29 +/- 0.08	1.54 +/- 0.11	1.30 +/-0.05	1.50 +/- 0.05	1.17 +/- 0.01
Fucose	0.32 +/- 0.12	0.30 +/- 0.09	0.41 +/- 0.00	0.35 +/- 0.10	0.25 +/- 0.05	0.33 +/- 0.04
Arabinose	2.90 +/- 0.28	2.89 +/- 0.27	3.04 +/- 0.03	3.57 +/- 0.41	2.72 +/- 0.07	3.36 +/- 0.13
Xylose	27.96 +/- 0.54	28.36 +/- 0.02	29.37 +/- 0.27	31.16 +/- 0.44	28.30 +/- 1.09	28.62 +/- 0.01
Glucose	60.67 +/- 0.42	60.46 +/-0.12	61.90 +/- 0.12	60.05 +/- 0.81	61.31 +/- 1.18	59.45 +/- 0.33
Galactose	2.94 +/- 0.58	3.18 +/- 0.24	3.74 +/- 0.52	3.58 +/- 0.20	2.49 +/- 0.04	3.15 +/- 0.09
Mannose	**3.97 +/- 0.45**	**3.52 +/- 0.19**	**0.00 +/- 00**	**0.00 +/- 00**	**3.44 +/- 0.07**	**3.91 +/- 0.05**

WT: Wild type Arabidopsis (Col0) WT1 and WT2 are two different plants; TM: triple mutant *csld2/csld3/csld5* TM1 and TM2 are two different plants; 71 and 72: two independent lines corresponding to the TM transformed with *proIrx5::TaCslA12*. Average values and standard deviation from technical replicates.

Acknowledgments

The authors acknowledge JC Helleisen and B. Rolland (INRAE Le Rheu) for growing wheat, L. Helary for technical help, M. Fanuel for training on the rapifleX and M. Francin-Allami for providing the BIFC vectors.

Funding

YV received funding from the European Union through the 7th Framework Program for research and the Horizon 2020 Research and Innovation Programme under the Marie Skłodowska-Curie [grant agreement No FP7-267196-MSCA-COFUND-AgreenSkills] and [H2020708329-MSCA-IF-2015]. The Maldi-Tof MS experiment was conducted using the equipment of the BIBS facility in Nantes (UR1268 BIA, IBiSA, Phenome-Emphasis-FR [grant number ANR-11-INBS-0012]).

The mannan research at the Institute for Plant Cell Biology and Biotechnology, Düsseldorf, is funded by the Deutsche Forschungsgemeinschaft (DFG, German Research Foundation) under Germany's Excellence Strategy – EXC 2048/1 – [Project ID: 390686111] and Deutsche Forschungsgemeinschaft (DFG, German Research Foundation) [grant PA 1366/1-1]. C.V. is supported by the DFG Research Grant [Project ID: 414353267].

Work by the DOE Joint BioEnergy Institute (http://www.jbei.org) was supported by the U. S. Department of Energy, Office of Science, Office of Biological and Environmental Research, through contract [DE-AC02-05CH11231] between Lawrence Berkeley National Laboratory and the U. S. Department of Energy.

Figures

Fig. 1. Immunodetection of mannan at early stages of wheat grain development. Micrographs of transverse sections from representative samples of wheat grain at the cellularization stage from 75°DAF to 150°DAF (for subsequent stages see Fig.S1B). Left: tissue organization showed by staining with toluidine blue. Right: fluorescence immunolabeling experiments carried out using the antibody LM21, which recognizes mannan and mannooligosaccharides. The annotated red squares in left panels represent the area imaged in right panels. Zoom in the region within the square shows details about endosperm cells (the arrow points to a sign of mitose). P: pericarp; np: nucellar projection; ne: nucellar epidermis; e: endosperm; ca: cavity; v: ventral side; d: dorsal side.

Fig. 2. Subcellular localization of TaCslA7, TaCslA12 and TaCslD2. Agroinfiltration of *Nicotiana tabacum* leaves with TaCslA7 or TaCslA12 or TaCslD2 fused with a fluorescent protein and co-transformation with the Golgi marker (sialyltransferase (ST)) or ER marker dihydrosphingosine phosphate lyase 1 (DPL1) fused with a fluorescent protein. Left panels: images showing fluorescence associated to the GFP, middle panel; fluorescence associated to the RFP and right panels: merge images with both signals showing co-localization. Bottom : co-expression TaCslA12-GFP/TaCslD2-RFP (two independent assays). The arrows point to co-localization. Scale bar: 10 µm.

Fig. 3. Analysis of *Pichia pastoris* lines expressing plant *CslA* genes. A Enzymatic quantification of mannan in Pichia wall. Pichia cell wall Alkaline-Insoluble (AKI) polysaccharides were treated with β-1,4-mannanase. Percentage of hexose sugars solubilized were quantified using the anthrone assay. Data show the mean + SD of three biological replicates. Different letters denote significant changes based on one-way ANOVA with post-hoc Tukey HSD Test ($P < 0.01$). B Glycosidic linkage analysis of Pichia wall AKI. Values represent the percentage of total carbohydrate area detected. Ak – *Amorphophallus konjac*. Data show the mean + SD of three biological replicates. The other glycosidic linkages are shown in Supplementary Fig.S5. For linkage, different letters denote significant changes based on one-way ANOVA with post-hoc Tukey HSD Test ($P < 0.01$).

Fig. 4. Analysis of *Arabidopsis thaliana* lines expressing wheat *CslA* genes: HPAEC profiling. Chromatograms showing elution profiles of mannose, mannooligosaccharides (MOS), mannanase treated konjac glucomannan and alcohol insoluble residues obtained from Arabidopsis stems. The resulting mannose and oligosaccharides were separated by HPAEC on a Carbo-Pac PA1 column. The same amount of alcohol insoluble residues was used for WT, the *csld2/csld3/csld9* (TM) mutant and TM transformed with pro*Irx5*::*TaCslA12* (71.1 and 72.1). M1: mannose; M2: mannobiose; M3: mannotriose; M4: mannotetraose; M5: mannopentaose; M6: mannohexaose; GM: glucomannan.

Fig. 5. Mass spectrometry profiles of alcohol insoluble residues obtained from Arabidopsis stems treated with endo-mannanase. The same amount of alcohol insoluble residues was used for WT and the *csld2*/*csld3*/*csld9* mutant transformed with pro*Irx5::TaCslA12* (72.1). Arrows: indicate a mass of 162 corresponding to anhydro-hexose. Red stars: indicate the number of acetyl groups on oligo-hexoses.

References

[1] T. Evers, S. Millar, Cereal grain structure and development: some implications for quality, J. Cereal Sci. 36 (2002) 261-284.

[2] Y. Xurun, C. Xinyu, Z. Liang, Z. Jing, Y. Heng, S. Shanshan, X. Fei, W. Zhong, Structural development of wheat nutrient transfer tissues and their relationships with filial tissues development, Protoplasma 252 (2015) 605-617.

[3] A.L. Chateigner-Boutin, B. Bouchet, C. Alvarado, B. Bakan, F. Guillon F, The wheat grain contains pectic domains exhibiting specific spatial and development-associated distribution, PLoS One 9 (2014) (2):e89620.

[4] G. Gartaula, S. Dhital, G. Netzel, B.M. Flanagan, G.E. Yakubov, C.T. Beahan, H.M. Collins, R.A. Burton, Bacic A, M.J. Gidley, Quantitative structural organisation model for wheat endosperm cell walls: Cellulose as an important constituent, Carbohydr. Polym. 196 (2018) 199-208.

[5] Y. Verhertbruggen, X. Falourd, M. Sterner, F. Guillon, C. Girousse, L. Foucat, S. Le Gall, A.L. Chateigner-Boutin, L. Saulnier, Challenging the putative structure of mannan in wheat (Triticum aestivum) Endosperm. Carbohyd. Polymer 224 (2019) 115063.

[6] L. Saulnier, F. Guillon, A.L. Chateigner-Boutin, Cell wall deposition and metabolism in wheat grain, Journal of Cereal Science 56 (2012) 91-108.

[7] H.V. Scheller, P. Ulvskov, Hemicelluloses, Annu. Rev. Plant Biol. 61 (2010) 263-289.

[8] M. Pauly, S. Gille, L. Liu, N. Mansoori, A. de Souza, A. Schultink, G. Xiong, Hemicellulose biosynthesis, Planta 238 (2013) 627-642.

[9] B. Gómez, B. Míguez, R. Yáñez, J.L. Alonso, Manufacture and properties of glucomannans and glucomannooligosaccharides derived from konjac and other sources, J. Agric. Food. Chem. 65 (2017) 2019-2031.

[10] L. Pitkänen, P. Tuomainen, K. Mikkonen, M. Tenkanen, The effect of galactose side units and mannan chain length on the macromolecular characteristics of galactomannans, Carbohyd. Polymers 86 (2011) 1230-1235.

[11] L. Yu, J.J. Lyczakowski, C.S. Pereira, T. Kotake, X. Yu, A. Li, S. Mogelsvang, M.S. Skaf, P. Dupree, The patterned structure of galactoglucomannan suggests it may bind to cellulose in seed mucilage, Plant Physiol. 178 (2018) 1011-1026.

[12] Mdel C. Rodríguez-Gacio, R. Iglesias-Fernández, P. Carbonero, A.J. Matilla, Softening-up mannan-rich cell walls. J. Exp. Bot. 63 (2012) 3976-3988.

[13] F. Grimaud, S. Pizzut-Serin, L. Tarquis, S. Ladevèze, S. Morel, J.L. Putaux, G. Potocki-Veronese, In vitro synthesis and crystallization of β-1,4-Mannan, Biomacromolecules 20 (2019) 846-853.

[14] D.H. Northcote, J.D. Pickett-Heaps, A function of the Golgi apparatus in polysaccharide synthesis and transport in the root-cap cells of wheat, Biochem. Journal 98 (1966)159-167.

[15] K.S. Dhugga, R. Barreiro, B. Whitten, K. Stecca, J. Hazebroek, G.S. Randhawa, M. Dolan, A.J. Kinney, D. Tomes, S. Nichols, P. Anderson, Guar seed beta-mannan synthase is a member of the cellulose synthase super gene family, Science 303 (2004) 363-366.

[16] A.H. Liepman, D.M. Cavalier, The CELLULOSE SYNTHASE-LIKE A and CELLULOSE SYNTHASE-LIKE C families: recent advances and future perspectives, Front. Plant Sci. 3 (2012)109.

[17] F. Goubet, A. Misrahi, S.K. Park, Z. Zhang, D. Twell, P. Dupree, AtCSLA7, a cellulose synthase-like putative glycosyltransferase, is important for pollen tube growth and embryogenesis in Arabidopsis, Plant Physiol 131 (2003) 547-557.

[18] Y. Verhertbruggen, L. Yin, A. Oikawa, H.V. Scheller, Mannan synthase activity in the CSLD family, Plant Signal Behav. 6 (2011) 1620-1623.

[19] L. Yin, Y. Verhertbruggen, A. Oikawa, C. Manisseri, B. Knierim, L. Prak, J.K. Jensen, J.P. Knox, M. Auer, W.G. Willats, H.V. Scheller, The cooperative activities of CSLD2, CSLD3, and CSLD5 are required for normal Arabidopsis development, Mol. Plant 4 (2011) 1024-1037.

[20] Y. Yin, M.A. Johns, H. Cao, M. Rupani, A survey of plant and algal genomes and transcriptomes reveals new insights into the evolution and function of the cellulose synthase superfamily, BMC Genomics 15 (2014) 260.

[21] M.E. Edwards, E. Marshall, M.J. Gidley, J.S. Reid, Transfer specificity of detergent-solubilized fenugreek galactomannan galactosyltransferase, Plant Physiol 129 (2002) 1391-1397.

[22] C. Voiniciuc, M.H.-W. Schmidt, A. Berger, B. Yang, B. Ebert, H.V. Scheller, H.M. North, B. Usadel, M. Günl, MUCILAGE-RELATED10 produces galactoglucomannan that maintains pectin and cellulose architecture in arabidopsis seed mucilage, Plant Physiol. 169 (2015) 403–420.

[23] Y. Wang, J.C. Mortimer, J. Davis, P. Dupree, K. Keegstra, Identification of an additional protein involved in mannan biosynthesis, Plant J. 73 (2013) 105-117. doi:10.1111/tpj.12019

[24] C. Voiniciuc, M. Dama, N. Gawenda, F. Stritt, M. Pauly, Mechanistic insights from plant heteromannan synthesis in yeast, Proc. Natl. Acad. Sci. U S A 116 (2019) 522-527.

[25] R. Zhong, D. Cui, Z.H. Ye, Members of the DUF231 Family are O-acetyltransferases catalyzing 2-O- and 3-O-acetylation of mannan, Plant Cell Physiol 59 (2018) 2339-2349.

[26] A.H. Liepman, C.G. Wilkerson, K. Keegstra, Expression of cellulose synthase-like (Csl) genes in insect cells reveals that CslA family members encode mannan synthases, Proc. Natl. Acad. Sci. U S A 102 (2005) 2221-2226.

[27] S. Gille, A. de Souza, G. Xiong, M. Benz, K. Cheng, A. Schultink, I.B. Reca, M. Pauly, O-acetylation of Arabidopsis hemicellulose xyloglucan requires AXY4 or AXY4L, proteins with a TBL and DUF231 domain. Plant Cell 23 (2011) 4041-4053.

[28] S. Park, A.L. Szumlanski, F. Gu, F. Guo, E. Nielsen, A role for CSLD3 during cell-wall synthesis in apical plasma membranes of tip-growing root-hair cells, Nat. Cell Biol. 13 (2011) 973-980.

[29] J. Yang J., G. Bak, T. Burgin, W.J. Barnes, H.B. Mayes, M.J. Peña, B.R. Urbanowicz, E. Nielsen, Biochemical and genetic analysis identify CSLD3 as a beta-1,4-glucan synthase that functions during plant cell wall synthesis, Plant Cell 32 (2020) 1749-1767.

[30] T.K. Pellny, A. Lovegrove, J. Freeman, P. Tosi, C.G. Love, J.P. Knox, P.R., Shewry, R.A. Mitchell, Cell walls of developing wheat starchy endosperm: comparison of composition and RNA-Seq transcriptome, Plant Physiol. 158 (2012) 612-627.

[31] C. Nemeth, J. Freeman, H.D. Jones, C. Sparks, T.K. Pellny, M.D. Wilkinson, J. Dunwell, A.A. Andersson, P. Aman, F. Guillon, L. Saulnier, R.A. Mitchell, P.R. Shewry, Down-regulation of the CSLF6 gene results in decreased (1,3;1,4)-beta-D-glucan in endosperm of wheat, Plant Physiol. 152 (2010) 1209-1218.

[32] D. Capron, S. Mouzeyar, A. Boulaflous, C. Girousse, C. Rustenholz, C. Laugier, E. Paux, M. Bouzidi, Transcriptional profile analysis of E3 ligase and hormone-related genes expressed during wheat grain development, BMC Plant Biology 12 (2012).

[33] M. Suliman M, A.L. Chateigner-Boutin, M. Francin-Allami, A. Partier, B. Bouchet, J. Salse, C. Pont, J. Marion, H. Rogniaux, D. Tessier, F. Guillon, C. Larré, Identification of glycosyltransferases involved in cell wall synthesis of wheat endosperm, J. Proteomics 78 (2013) 508-521.

[34] M. Cherkaoui, V. Lollier, A. Geairon, A. Bouder, C. Larré, H. Rogniaux, E. Jamet, F. Guillon, M. Francin-Allami, Cell wall proteome of wheat grain endosperm and outer layers at two key stages of early development, Int. J. Mol. Sci. 21 (2019) 239.

[35] B. Li, J. Xia, Y. Wang, B. Xie, Grain-size effect on the structure and antiobesity activity of konjac flour, J. Agr. Food Chem. 53 (2005) 7404-7407.

[36] H. Joshi, V. Kapoor, Cassia grandis Linn. f. seed galactomannan: structural and crystallographical studies, Carbohydr. Res. 338 (2003) 1907-1912.

[37] M.S. Buckeridge, Seed cell wall storage polysaccharides: models to understand cell wall biosynthesis and degradation, Plant Physiol. 154 (2010) 1017-1023.

[38] L. Moreira, E. Filho, An overview of mannan structure and mannan-degrading enzyme systems, Appl. Microbiol. Biotechnol. 79 (2008) 165-178.

[39] Y. Liang, A. Eudes, S. Yogiswara, B. Jing, V. Benites, R. Yamanaka, C. Cheng-Yue, E. Baidoo, J. Mortimer, H. Scheller, D. Loque, A screening method to identify efficient sgRNAs in Arabidopsis, used in conjunction with cell-specific lignin reduction. Biotechnol. Biofuels 12 (2019).

[40] A.L. Chateigner-Boutin, J. Ordaz-Ortiz, C. Alvarado, B. Bouchet, S. Durand, Y. Verhertbruggen, Y. Barriere, L. Saulnier, Developing Pericarp of Maize: A Model to Study Arabinoxylan Synthesis and Feruloylation, Front. Plant Sci. 7 (2016).

[41] S. Marcus, A. Blake, T. Benians, K. Lee, C. Poyser, L. Donaldson, O. Leroux, A. Rogowski, H. Petersen, A. Boraston, H. Gilbert, W. Willats, J.P. Knox, Restricted access of proteins to mannan polysaccharides in intact plant cell walls, Plant J. 64 (2010) 191-203.

[42] M. Mutwil, S. Klie, T. Tohge, F.M. Giorgi, O. Wilkins, M.M. Campbell, A.R. Fernie, B. Usadel, Z. Nikoloski, S. Persson, PlaNet: combined sequence and expression comparisons across plant networks derived from seven species, Plant Cell 23 (2011) 895-910.

[43] R.H. Ramírez-González, P. Borrill, D. Lang, S.A. Harrington, J. Brinton, L. Venturini, M. Davey, J. Jacobs, F. van Ex, A. Pasha, Y. Khedikar, S.J. Robinson, A.T. Cory, T. Florio, L. Concia, C. Juery, H. Schoonbeek, B. Steuernagel, D. Xiang, C.J. Ridout, B. Chalhoub, K.F.X. Mayer, M. Benhamed, D. Latrasse, A. Bendahmane, B.B.H. Wulff, R. Appels, V. Tiwari, R. Datla, F. Choulet, C.J. Pozniak, N.J. Provart, A.G. Sharpe, E. Paux, M. Spannagl, A. Bräutigam, C. Uauy, Consortium IWGS, The transcriptional landscape of polyploid wheat, Science 361 (2018) 6403.

[44] P. Borrill, R. Ramirez-Gonzalez, C. Uauy, expVIP: a customizable RNA-seq data analysis and visualization platform, Plant Physiol. 170 (2016) 2172-2186.

[45] I. Sparkes, J. Runions, A. Kearns, C. Hawes, Rapid, transient expression of fluorescent fusion proteins in tobacco plants and generation of stably transformed plants, Nat. Protoc. 1 (2006) 2019-2025.

[46] M. Nishikawa, K. Hosokawa, M. Ishiguro, H. Minamioka, K. Tamura, I. Hara-Nishimura, Y. Takahashi, K. Shimazaki, H. Imai, Degradation of sphingoid long-chain base 1-phosphates (LCB-1Ps): functional characterization and expression of AtDPL1 encoding LCB-1P lyase involved in the dehydration stress response in Arabidopsis, Plant Cell Physiol. 49 (2008) 1758-1763.

[47] J. Azimzadeh, P. Nacry, A. Christodoulidou, S. Drevensek, C. Camilleri, N. Amiour, F. Parcy, M. Pastuglia, D. Bouchez, Arabidopsis TONNEAU1 proteins are essential for preprophase band formation and interact with centrin, Plant Cell 20 (2008) 2146-2159.

[48] Z. Schwarz-Sommer, I. Hue, P. Huijser, P.J. Flor, R. Hansen, F. Tetens, W.E. Lönnig, H. Saedler, H. Sommer, Characterization of the Antirrhinum floral homeotic MADS-box gene deficiens: evidence for DNA binding and autoregulation of its persistent expression throughout flower development, EMBO J 11 (1992) 251-263.

[49] J. Lin-Cereghino J, W. Wong, S. Xiong, W. Giang, L. Luong, J. Vu, S. Johnson, G. Lin-Cereghino, Condensed protocol for competent cell preparation and transformation of the methylotrophic yeast *Pichia pastoris*, Biotechniques 38 (2005) 44.

[50] C. Voiniciuc, M. Günl, Analysis of monosaccharides in total mucilage extractable from Arabidopsis seeds, Bio-protocol 6 (2016) e1801.

[51] C.E. Foster, T.M. Martin, M. Pauly, Comprehensive compositional analysis of plant cell walls (lignocellulosic biomass) Part II: Carbohydrates, J. Vis. Exp. 37 (2010) e1745.

[52] I. Ciucanu, F. Kerek, A simple and rapid method for the permethylation of carbohydrates, Carbohydr. Res. 131 (1984) 209–217.

[53] I. Ciucanu, Per-O-methylation reaction for structural analysis of carbohydrates by mass spectrometry, Anal. Chim. Acta 576 (2006) 147–155.

[54] A. Himmelbach, U. Zierold, G. Hensel, J. Riechen, D. Douchkov, P. Schweizer, J. Kumlehn, A set of modular binary vectors for transformation of cereals, Plant Physiol. 145 (2007) 1192-1200.

[55] A. Eudes, A. George, P. Mukerjee, J.S. Kim, B. Pollet, P.I. Benke, F. Yang, P. Mitra, L. Sun, O.P. Cetinkol, S. Chabout, G. Mouille, L. Soubigou-Taconnat, S. Balzergue, S. Singh, B.M. Holmes, A. Mukhopadhyay, J.D. Keasling, B.A. Simmons, C. Lapierre, J. Ralph, D. Loqué, Biosynthesis and incorporation of side-chain-truncated lignin monomers to reduce lignin polymerization and enhance saccharification, Plant Biotechnol. J 10 (2012) 609-620.

[56] S.J. Clough, A.F. Bent, Floral dip: a simplified method for Agrobacterium-mediated transformation of Arabidopsis thaliana, Plant J. 16 (1998) 735-743.

[57] Y. Zou, M. Mason, Y. Wang, E. Wee, C. Turni, P. Blackall, M. Trau, J. Botella, Nucleic acid purification from plants, animals and microbes in under 30 seconds, Plos Biology 15 (2017) (11).

[58] H. Englyst, J. Cummings, Improved method of measurement of dietary fiber as non-starch polysaccharides in plant foods, J Assoc Off Anal Chem 71 (1988) 808-814.

[59] N. Yacoubi, F. Van Immerseel, R. Ducatelle, L. Rhayat, E. Bonnin, L. Saulnier, Water-soluble fractions obtained by enzymatic treatment of wheat grains promote short chain fatty acids production by broiler cecal microbiota, Anim. Feed Sci. Tech. 218 (2016) 110-119.

[60] D. Mares, B. Stone, Studies on wheat endosperm. I. Chemical composition and ultrastructure of the cell walls, Aust. J. Biol. Sci. 23 (1974) 793-812.

[61] A.L. Chateigner-Boutin, M. Suliman, B. Bouchet, C. Alvarado, V. Lollier, H. Rogniaux, F. Guillon, C. Larré, Endomembrane proteomics reveals putative enzymes involved in cell wall metabolism in wheat grain outer layers, J. Exp. Bot. 66 (2015) 2649-2658.

[62] R. Palmer, V. Cornuault, S.E. Marcus, J.P. Knox, P.R. Shewry, P. Tosi, Comparative in situ analyses of cell wall matrix polysaccharide dynamics in developing rice and wheat grain, Planta 241 (2015) 669-685.

[63] M. Francin-Allami, C. Alvarado, S. Daniel, A. Geairon, L. Saulnier, F. Guillon, Spatial and temporal distribution of cell wall polysaccharides during grain development of *Brachypodium distachyon*, Plant Sci. 280 (2019) 367-382.

[64] J.S. Kim, G. Daniel, Immunolocalization of hemicelluloses in *Arabidopsis thaliana* stem. Part II: Mannan deposition is regulated by phase of development and its patterns of temporal and spatial distribution differ between cell types, Planta 236 (2012) 1367-1379.

[65] Z. Fulton, A. McAlister, M.C. Wilce, R. Brammananth, L. Zaker-Tabrizi, M.A. Perugini, S.P. Bottomley, R.L. Coppel, P.K. Crellin, J. Rossjohn, T. Beddoe, Crystal structure of a UDP-glucose-specific glycosyltransferase from a Mycobacterium species, J. Biol. Chem. 283 (2008) 27881-27890.

[66] F. Goubet, A. Misrahi, S.K. Park, Z. Zhang, D. Twell, P. Dupree, AtCSLA7, a cellulose synthase-like putative glycosyltransferase, is important for pollen tube growth and embryogenesis in Arabidopsis, Plant Physiol. 131 (2003) 547-557.

[67] M.G. Handford, T.C. Baldwin, F. Goubet, T.A. Prime, J. Miles, X. Yu, P. Dupree, Localisation and characterisation of cell wall mannan polysaccharides in Arabidopsis thaliana, Planta 218 (2003) 27-36.

[68] S. Philippe, L. Saulnier, F. Guillon, Arabinoxylan and (1-->3),(1-->4)-beta-glucan deposition in cell walls during wheat endosperm development, Planta 224 (2006) 449-461.

[79] P. Robert, F. Jamme, C. Barron, B. Bouchet, L. Saulnier, P. Dumas, F. Guillon, Change in wall composition of transfer and aleurone cells during wheat grain development, Planta 233 (2011) 393-406.

[70] A.J. Bernal, C.M. Yoo, M. Mutwil, J.K. Jensen, G. Hou, C. Blaukopf, I. Sørensen, E.B. Blancaflor, H.V. Scheller, W.G. Willats, Functional analysis of the cellulose synthase-like genes CSLD1, CSLD2, and CSLD4 in tip-growing Arabidopsis cells, Plant Physiol, 148 (2008) 1238-1253.

[71] G. Qi, R. Hu, L. Yu, G. Chai, Y. Cao, R. Zuo, Y. Kong, G. Zhou, Two poplar cellulose synthase-like D genes, PdCSLD5 and PdCSLD6, are functionally conserved with Arabidopsis CSLD3, J. Plant Physiol. 170 (2013) 1267-1276.

[72] H. Hu, R. Zhang, S. Dong, Y. Li, C. Fan, Y. Wang, T. Xia, P. Chen, L. Wang, S. Feng, S. Persson, L. Peng, AtCSLD3 and GhCSLD3 mediate root growth and cell elongation downstream of the ethylene response pathway in Arabidopsis, J. Exp. Bot. 69 (2018) 1065-1080.

[73] H. Hu, R. Zhang, Y. Tang, C. Peng, L. Wu, S. Feng, P. Chen, Y. Wang, X. Du, L. Peng, Cotton CSLD3 restores cell elongation and cell wall integrity mainly by enhancing primary cellulose production in the Arabidopsis cesa6 mutant, Plant Mol. Biol. 101 (2019) 389-401.

[74] T.A. Richmond, C.R. Somerville, The cellulose synthase superfamily, Plant Physiol. 124 (2000) 495-498.

[75] L. Wang, K. Guo, Y. Li, Y. Tu, H. Hu, B. Wang, X. Cui, L. Peng, Expression profiling and integrative analysis of the CESA/CSL superfamily in rice, BMC Plant Biology 10 (2010).

[76] S. Kaur, K.S. Dhugga, R. Beech, J. Singh, Genome-wide analysis of the cellulose synthase-like (Csl) gene family in bread wheat (*Triticum aestivum* L.), BMC Plant Biol 17 (2017) 193.

[77] A. Little A, J.G. Schwerdt, N.J. Shirley, S.F. Khor, K. Neumann, L.A. O'Donovan, J. Lahnstein, H.M. Collins, M. Henderson, G.B. Fincher, R.A. Burton, Revised phylogeny of the cellulose synthase gene superfamily: insights into cell wall evolution, Plant Physiol 177 (2018) 1124-41.

[78] A. Jozwiak, P.D. Sonawane, S. Panda, C. Garagounis, K.K. Papadopoulou, B. Abebie, H. Massalha, E. Almekias-Siegl, T. Scherf, A. Aharoni, Plant terpenoid metabolism co-opts a component of the cell wall biosynthesis machinery, Nat. Chem. Biol. 16 (2020) 740–748.

[79] M. Atmodjo, Y. Sakuragi, X. Zhu, A. Burrell, S. Mohanty, J. Atwood, R. Orlando, H. Scheller, D. Mohnen, Galacturonosyltransferase (GAUT)1 and GAUT7 are the core of a plant cell wall pectin biosynthetic homogalacturonan: galacturonosyltransferase complex, Proc. Natl. Acad. Sci. U. S. A. 108 (2011) 20225-20230.

[80] J. Harholt, J.K. Jensen, Y. Verhertbruggen, C. Søgaard, S. Bernard, M. Nafisi, C.P. Poulsen, N. Geshi, Y. Sakuragi, A. Driouich, J.P. Knox, H.V. Scheller, ARAD proteins associated with pectic Arabinan biosynthesis form complexes when transiently overexpressed in planta, Planta 236 (2012) 115-128.

[81] Y. Chou, G. Pogorelko, Z. Young, O. Zabotina, Protein-Protein Interactions Among xyloglucan-synthesizing enzymes and formation of golgi-localized multiprotein complexes, Plant Cell Physiol. 56 (2015) 255-267.

[82] N. Jiang, R. Wiemels, A. Soya, R. Whitley, M. Held, A. Faik, Composition, assembly, and trafficking of a wheat xylan synthase complex, Plant Physiol. 170 (2016) 1999-2023.

[83] J. Hill, M. Hammudi, M. Tien, The Arabidopsis cellulose synthase complex: a proposed hexamer of CESA trimers in an equimolar stoichiometry, Plant Cell 26 (2014) 4834-4842.

[84] R. Amos, D. Mohnen, Critical review of plant cell wall matrix polysaccharide glycosyltransferase activities verified by heterologous protein expression, Front. Plant Sci. 10 (2019).

[85] C. Kim, S. Park, B. Il Je, S. Park, H. Piao, M. Eun, L. Dolan, C. Han C, OsCSLD1, a cellulose synthase-like D1 gene, is required for root hair morphogenesis in rice, Plant Physiol. 143 (2007) 1220-1230.

[86] W. Li, Z. Yang, J. Yao, J. Li, W. Song, X. Yang, Cellulose synthase-like D1 controls organ size in maize. BMC Plant Biol. 18 (2018).

[87] F. Gu, M. Bringmann, J. Combs, J. Yang, D. Bergmann, E. Nielsen, Arabidopsis CSLD5 Functions in Cell Plate Formation in a Cell Cycle-Dependent Manner, Plant Cell 28 (2016) 1722-1737.

[88] W. Luan, Y. Liu, F. Zhang, Y. Song, Z. Wang, Y. Peng, Z. Sun, OsCD1 encodes a putative member of the cellulose synthase-like D sub-family and is essential for rice plant architecture and growth, Plant Biotechnol. J. 9 (2011) 513-524.

[89] D. Douchkov, S. Lueck, G. Hensel, J. Kumlehn, J. Rajaraman, A. Johrde, M. Doblin, C. Beahan, M. Kopischke, R. Fuchs, V. Lipka, R. Niks, V. Bulone, J. Chowdhury, A. Little, R. Burton, A. Bacic, G. Fincher, P. Schweizer, The barley (*Hordeum vulgare*) cellulose synthase-like D2 gene (HvCslD2) mediates penetration resistance to host-adapted and nonhost isolates of the powdery mildew fungus, New Phytol. 212 (2016) 421-433.

[90] M. Hernandez-Gomez, J. Runavot, X. Guo, S. Bourot, T. Benians, W. Willats, F. Meulewaeter, J.P. Knox, Heteromannan and heteroxylan cell wall polysaccharides display different dynamics during the elongation and secondary cell wall deposition phases of cotton fiber cell development, Plant Cell Physiol. 56 (2015) 1786-1797.

[91] A. Chaudhury, T. Kaila, K. Gaikwad, Elucidation of galactomannan biosynthesis pathway genes through transcriptome sequencing of seeds collected at different developmental stages of commercially important indian varieties of cluster bean (*Cyamopsis tetragonoloba* L.), Sci. Rep. 9 (2019).

[92] G. Silva, M. Ionashiro, T. Carrara, A. Crivellari, M. Tine, J. Prado, N. Carpita, M. Buckeridge, Cell wall polysaccharides from fern leaves: Evidence for a mannan-rich Type III cell wall in *Adiantum raddianum*, Phytochem. 72 (2011) 2352-2360.

[93] M. Pauly, K. Keegstra, Plant cell wall polymers as precursors for biofuels, Curr. Opin. Plant Biol. 13 (2010) 305-312.

[94] O. Leroux, F. Leroux, A. Bagniewska-Zadworna, J.P. Knox, M. Claeys, S. Bals, R. Viane, Ultrastructure and composition of cell wall appositions in the roots of Asplenium (Polypodiales), Micron 42 (2011) 863-870.

[95] A. Benova-Kakosova, C. Digonnet, F. Goubet, P. Ranocha, A. Jauneau, E. Pesquet, O. Barbier, Z. Zhang, P. Capek, P. Dupree, D. Liskova, D. Goffner, Galactoglucomannans increase cell population density and alter the protoxylem/metaxylem tracheary element ratio in xylogenic cultures of zinnia, Plant Physiol. 142 (2006) 696-709.

[96] M. Marks, L. Betancur, E. Gilding, F. Chen, S. Bauer, J. Wenger, R. Dixon, C. Haigler, A new method for isolating large quantities of Arabidopsis trichomes for transcriptome, cell wall and other types of analyses, Plant J. 56 (2008) 483-492.

Fig.1.


75°DAF
200 µm
V
d
a
Zoom in d
20 µm
d

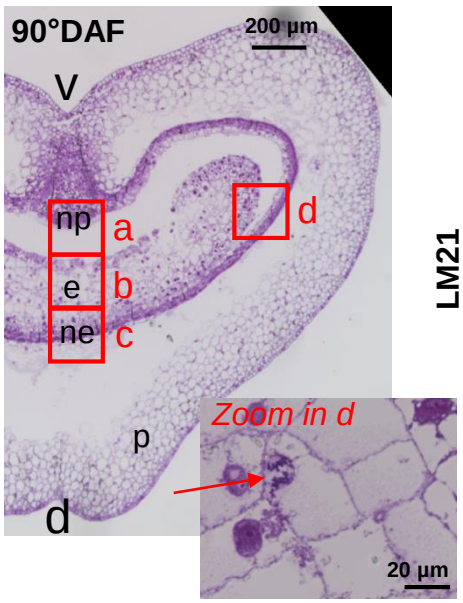
90°DAF
200 µm
V
np
a
d
e
b
ne
c
Zoom in d
p
20 µm
d

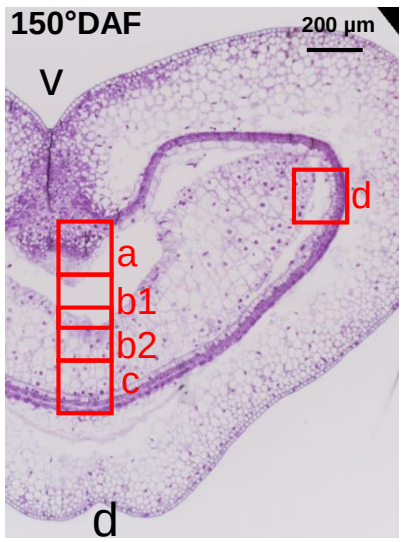
150°DAF
200 µm
V
d
a
b1
b2
c
d

LM21

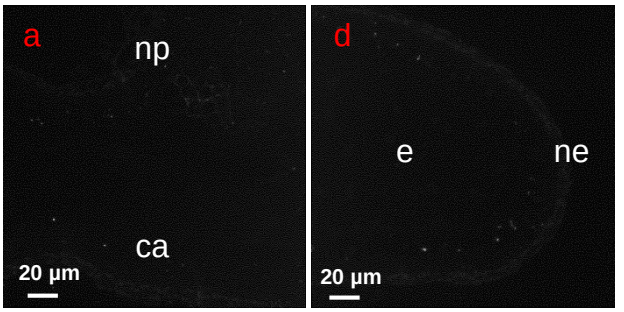
a
np
ca
20 µm
d
e
ne
20 µm

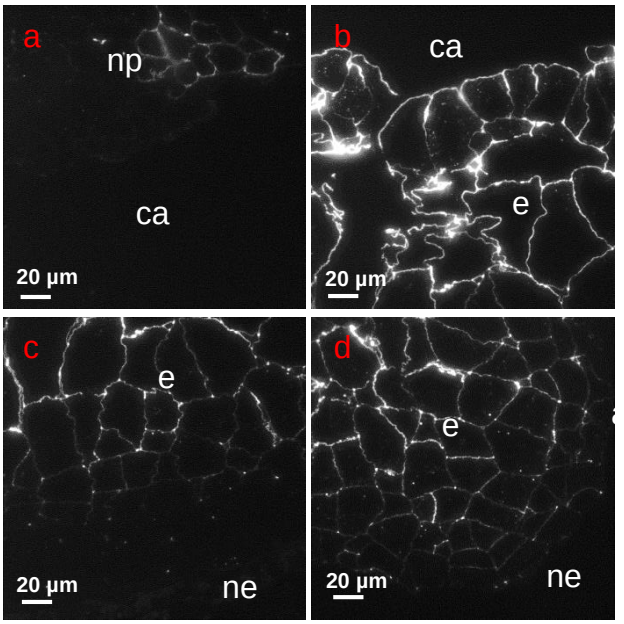
a
np
ca
20 µm
b
ca
e
20 µm
c
e
20 µm
ne
d
e
20 µm
ne

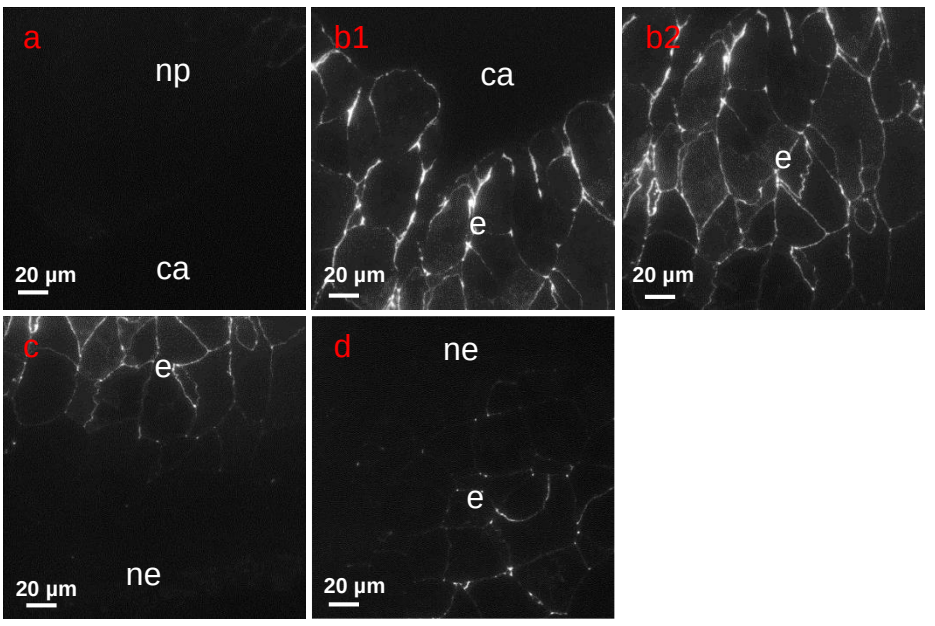
a
np
ca
20 µm
b1
ca
e
20 µm
b2
e
20 µm
c
e
ne
20 µm
d
ne
e
20 µm

Fig. 2.

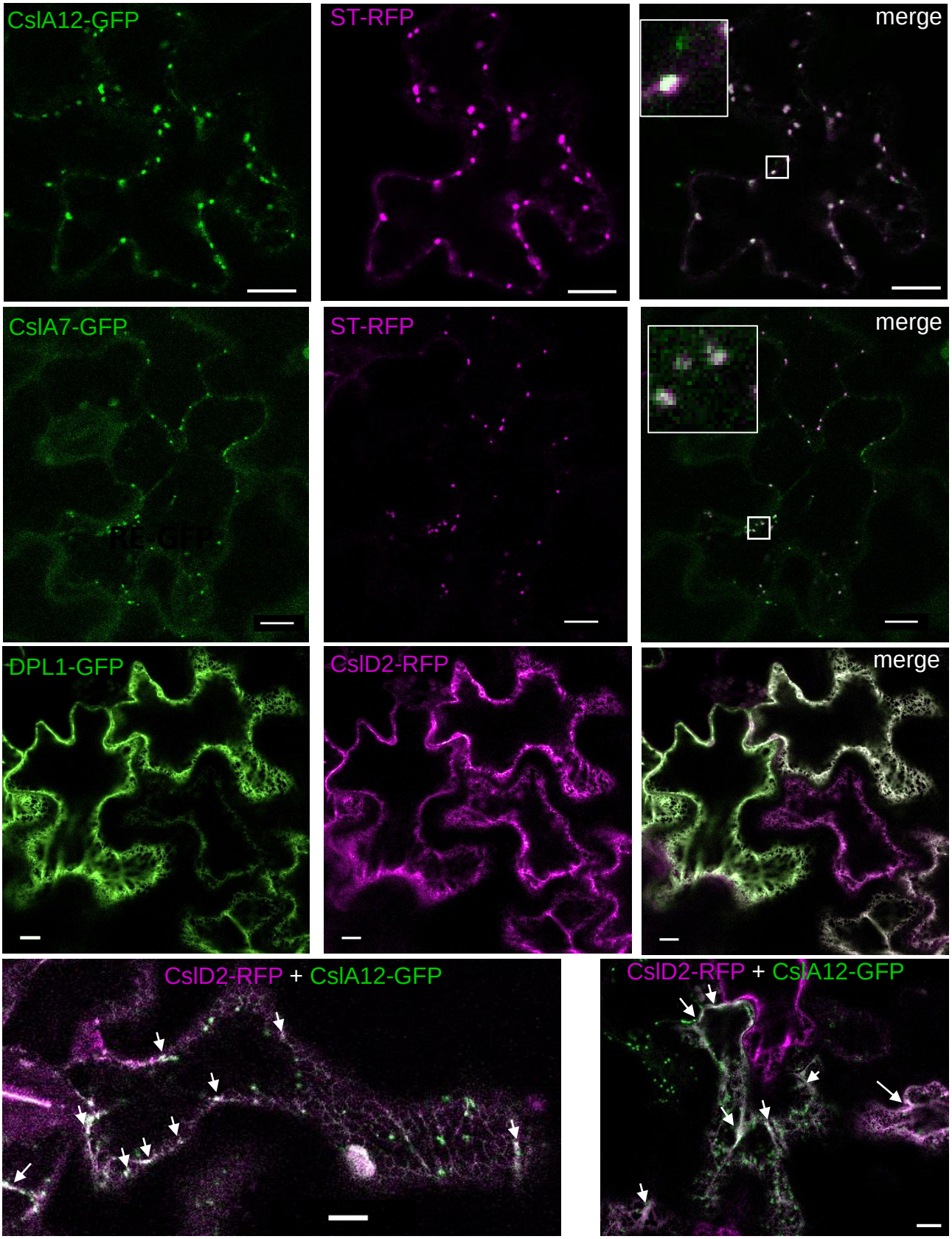
CslA12-GFP
ST-RFP
merge
CslA7-GFP
ST-RFP
merge
DPL1-GFP
CslD2-RFP
merge
CslD2-RFP + CslA12-GFP
CslD2-RFP + CslA12-GFP

Fig.3.

A

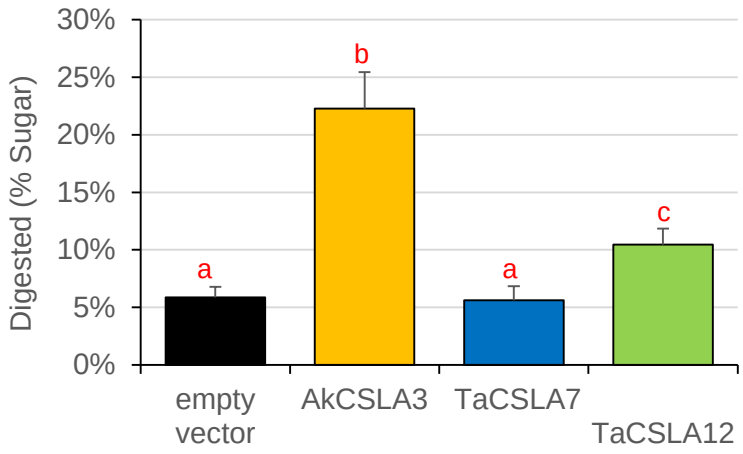
30%
25%
20%
15%
10%
5%
0%
Digested (% Sugar)
a
b
a
c
empty vector
AkCSLA3
TaCSLA7
TaCSLA12

B

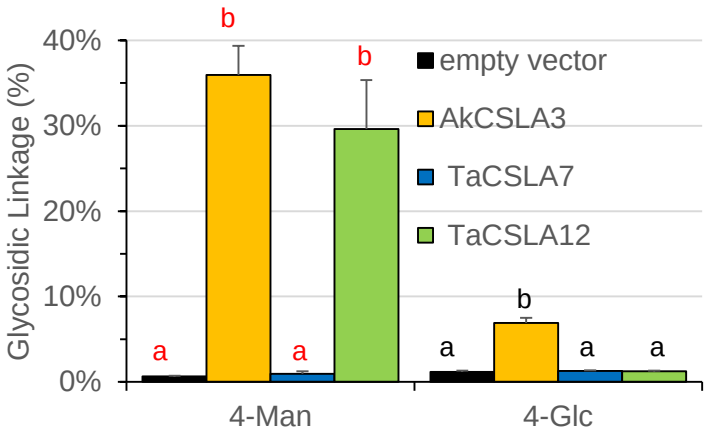
40%
30%
20%
10%
0%
Glycosidic Linkage (%)
a
b
a
b
a
b
a
a
empty vector
AkCSLA3
TaCSLA7
TaCSLA12
4-Man
4-Glc

Fig. 4.

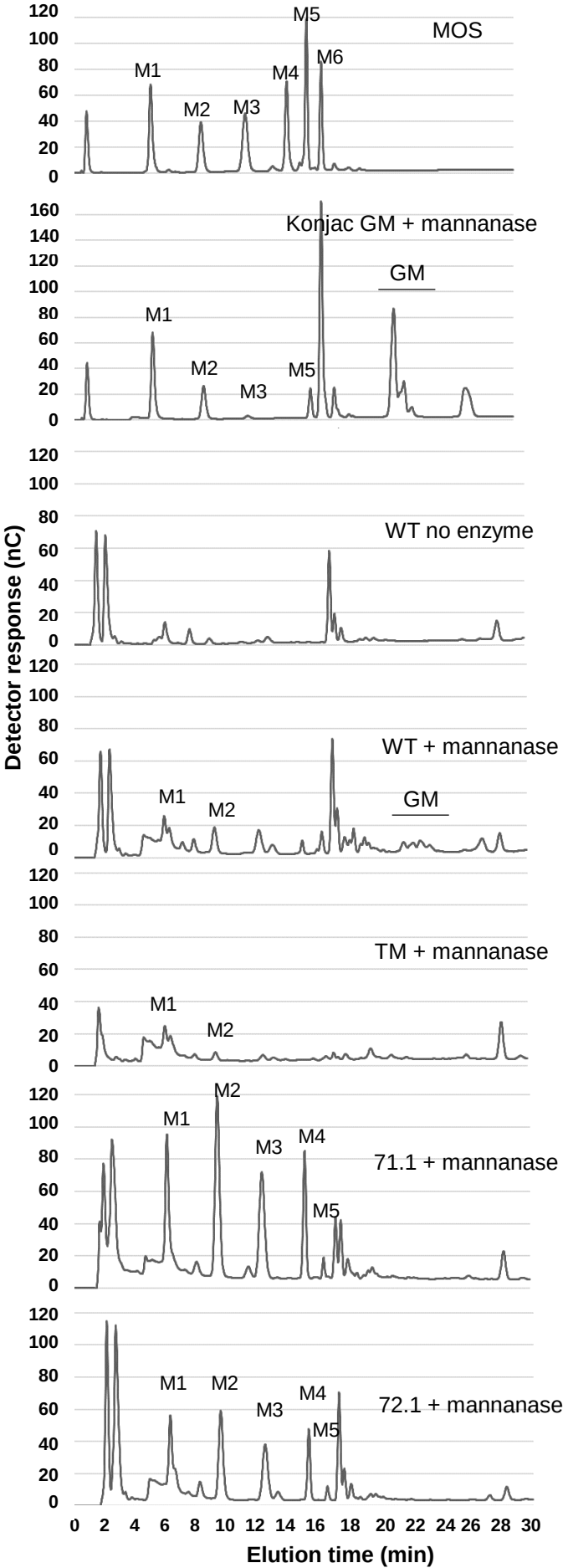
MOS
M1
M2
M3
M4
M5
M6
Konjac GM + mannanase
GM
WT no enzyme
WT + mannanase
TM + mannanase
71.1 + mannanase
72.1 + mannanase
Detector response (nC)
Elution time (min)

Fig. 5.

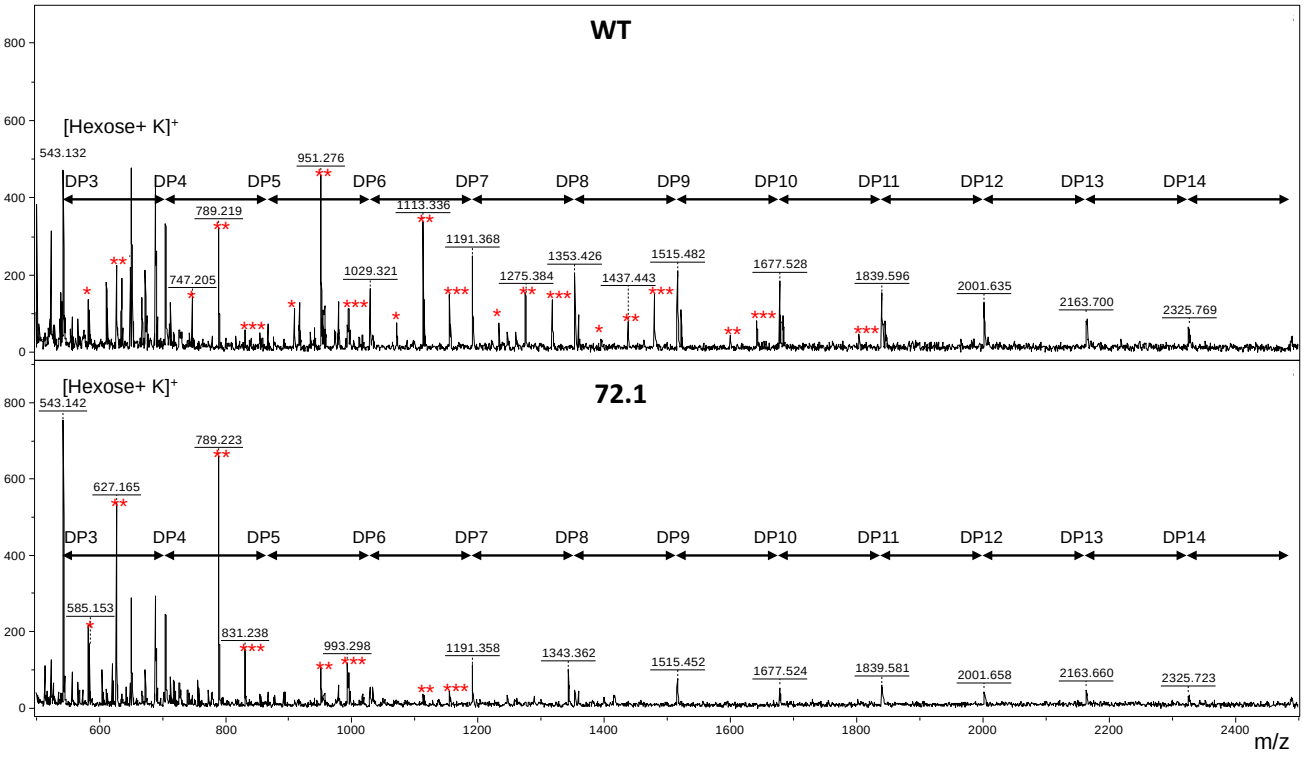
WT
[Hexose+ K]+
543.132
951.276
789.219
1113.336
1191.368
1353.426
1515.482
747.205
1029.321
1275.384
1437.443
1677.528
1839.596
2001.635
2163.700
2325.769
DP3
DP4
DP5
DP6
DP7
DP8
DP9
DP10
DP11
DP12
DP13
DP14
72.1
[Hexose+ K]+
543.142
789.223
627.165
585.153
831.238
993.298
1191.358
1343.362
1515.452
1677.524
1839.581
2001.658
2163.660
2325.723
0
200
400
600
800
600
800
1000
1200
1400
1600
1800
2000
2200
2400
m/z